Available online at www.sciencedirect.com
ScienceDirect
Trans. Nonferrous Met. Soc. China 32(2022) 1385−1404
Transactions of Nonferrous Metals Society of China
www.tnmsc.cn

Recent advances of electromagnetic interference shielding Mg matrix materials and their processings: A review

Jia-hao WANG[1], Rui-zhi WU[1,2], Jing FENG[1], Jing-huai ZHANG[1], Le-gan HOU[1], Mei-duo LIU[3]

1. Key Laboratory of Superlight Materials & Surface Technology, Ministry of Education, Harbin Engineering University, Harbin 150001, China;
2. College of Science, Heihe University, Heihe 164300, China;
3. Department of Environmental Engineering, Heilongjiang University of Technology, Jixi 158100, China

Received 11 August 2021; accepted 27 October 2021

Abstract: In terms of lightweight electromagnetic interference (EMI) shielding structural materials, Mg matrix materials have proven to be the best, due to their exciting properties (e.g. low density, high specific strength, good electrical conductivity and excellent EMI shielding properties) and their wide range of applications in lightweighting in electronics, automotive and aerospace industries. Through processing, such as alloying, heat treatment, plastic deformation and composite processing, Mg matrix materials can be obtained with tailorable properties which can play a key role in designing materials for EMI shielding. This work introduces an overview of the research on the EMI shielding properties of Mg matrix materials as well as their EMI shielding mechanisms over the past few decades, focused on the influence of alloying, heat treatment, plastic deformation and composite processing for the EMI shielding properties of Mg matrix materials. At the end, conclusions and future perspectives are provided.

Key words: magnesium; electromagnetic interference shielding; alloying; heat treatment; plastic deformation; composite processing

1 Introduction

Continuous development in the information technology, especially the rapid development of new electronic devices, such as portable mobile phones and computers, radar and communication satellites, has greatly improved the efficiency of social production and brought great convenience to citizens in their daily lives [1]. However, the frequent use of electronic devices has led to a proliferation of electromagnetic (EM) radiation with different wavelengths [2,3]. Electromagnetic interference (EMI) will not only cause serious impact on electronic equipment, instruments and communication signals, but also cause harm to human health and the environment, such as causing cancer, affecting the brain development of infants, damaging the DNA structure of the human body and causing the normal growth of plants, genetic mutations and even death [4,5]. The EM radiation pollution is becoming the fifth most prevalent pollution after air, water, noise, and solid waste of the world [6]. In order to minimize the problems caused by EM radiation pollution, countries around the world have developed standards and regulations to control and purify the EM environment [7,8]. The most effective measure to control EMI is EM shielding, of which the main purpose is to reduce the intensity of EM radiation within a safe range by suppressing the effects of radio frequency EM waves. The research on effective EMI shielding

Corresponding author: Rui-zhi WU, Tel/Fax: +86-451-82569890, E-mail: rzwu@hrbeu.edu.cn;
Le-gan HOU, Tel/Fax: 86-451-82569890, E-mail: houlegan@163.com
DOI: 10.1016/S1003-6326(22)65881-3

materials has become urgent. The main EMI shielding materials include metal materials, conductive polymers and coating materials. However, some of these materials have their own drawbacks that make it difficult to be further developed. For example, the high density of traditional metal materials limits their application in the production and assembly of some lightweight industrial equipment [9−11]. The preparation process of some polymers and coating materials is cumbersome and the strength is lower than industrial requirements, which limits their application in structural materials [12−15]. Therefore, the development of new EMI shielding materials with lightweight, low-cost and suitable mechanical properties has become an urgent problem to be solved.

Magnesium (Mg) is considered to be the best environmentally friendly material in the 21st century [16]. Mg and its alloys have a high potential for applications in the automobiles, biomedicine, aerospace and 3C products because of their low density, high specific strength and specific stiffness, and excellent biocompatibility as well as other characteristics [17]. In addition, Mg alloys are also potential EMI shielding materials. Much literature has reported the EMI shielding properties of Mg matrix materials through different processes such as alloying, heat treatment, plastic deformation and composite processing, and the corresponding EMI shielding mechanisms. In this work, the research progress of the EMI shielding properties of Mg matrix materials in the last two decades is reviewed, with focuses on four preparation processings, namely alloying, heat treatment, plastic deformation and composite processing. The influence of the obtained microstructure under the different processings on the EMI shielding properties is discussed in detail. Finally, the development trend of Mg matrix EMI shielding materials is prospected.

2 EMI shielding mechanism and measurement methods

2.1 Mechanism of shielding

Figure 1 shows the mechanism of EMI shielding. As EM waves impinge on the surface of the material, the free electrons on the surface will generate an anti-electric field to neutralize the striking from EM waves, which is called impedance mismatch. Due to the impedance mismatch, some of the EM waves are reflected, called as reflected wave [18]. Some of the remaining EM waves penetrate the shielding material, becoming transmitted wave. Some of the EM waves are subjected to being multiple reflected and transmitted between the two interfaces of the shielding material with continuous attenuation. Therefore, the EMI shielding mechanism of shielding materials includes three parts: the reflection loss of the surface of the material, the absorption loss of the material, and the multiple reflection loss inside the material [19].

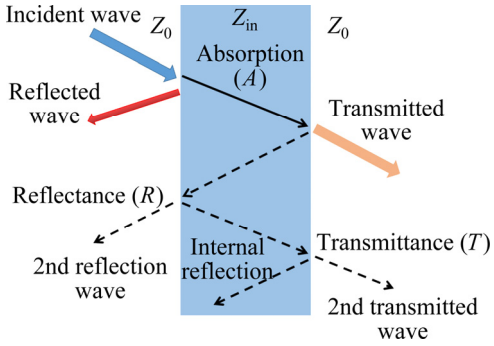

Fig.1 Mechanisms of EMI shielding

In order to quantitatively describe the shielding performance of shielding materials, shielding effectiveness (SE) is usually used to express the capability of an EMI shielding material in attenuation or reduction of EM signal, and the unit of SE is expressed in decibels (dB) [20]. In general, Schelkunoff formula is used to express the SE of an EMI shielding material [21]:

$$SE_T=SE_R+SE_A+SE_M=20\lg(E_t/E_i)= 20\lg(H_t/H_i)=10\lg(P_t/P_i) \quad (1)$$

where P_i (E_i or H_i) and P_t (E_t or H_t) are the power (electric or magnetic field intensity) of incident and transmitted EM waves, respectively [21]. Thus, the total SE of an EMI shielding material (SE_T) is the sum of three SE contributed from reflection (SE_R), absorption (SE_A), and multiple-internal reflections (SE_M). SE_M is negligible when SE_A is greater than 10 dB.

In addition, the propagation of EM waves through shielding material can also be described using power coefficients of transmissivity (T), reflectivity (R) and absorption (A), as shown in Eqs. (2) and (3) [22−24]:

$$T+R+A=1 \tag{2}$$

$$T=\frac{P_t}{P_i}=|S_{21}|^2,\ R=\frac{P_r}{P_i}=|S_{11}|^2,\ A=\frac{P_a}{P_i} \tag{3}$$

where P_r and P_a are the powers of reflected and absorbed EM waves, respectively. S_{11} is the scattering parameter related to the reflection coefficient and S_{21} is the scattering parameter related to the transmission coefficient. The effective absorbance (A_{eff}) can be described as follows [22−24]:

$$A_{eff}=\frac{A}{A+T} \tag{4}$$

Thus, the total shielding effectiveness SE_T, reflection loss SE_R and absorption loss SE_A can be expressed as [22−24]

$$SE_T=-10\lg T \tag{5}$$

$$SE_R=-10\lg(1-R) \tag{6}$$

$$SE_A=-10\lg(1-A_{eff}) \tag{7}$$

Several theories are used to calculate the SE of material, including plane-wave theory, metal foil, near field shielding, low-frequency magnetic field source, and scattering parameter [25]. Generally, EM waves radiated to a given shield can be approximated as plane waves. Therefore, plane-wave theory is the most commonly used for the calculation of SE [25]. For a plane-wave EM radiation, the total shielding effectiveness SE_T, reflection loss SE_R and absorption loss SE_A can be expressed as [26]

$$SE_T=SE_R+SE_A\ (SE_M \text{ is negligible}) \tag{8}$$

$$SE_R=39.5+10\lg\frac{\sigma}{2\pi f\mu} \tag{9}$$

$$SE_A=8.7\frac{d}{\delta}=8.7d\sqrt{\pi f\mu\sigma} \tag{10}$$

From the above functional relationship, it can be concluded that the balance of inherent physical properties including magnetic permeability (μ) and electrical conductivity (σ) is extremely important for achieving the required shielding.

2.2 Methods of EMI SE measurement

Accurate theoretical calculations of the EMI SE are usually relatively difficult. In practical applications, the EMI shielding properties of the material are often determined through measurements. EMI SE can be measured experimentally with instruments, called as network analyzers (NA), which can be divided into scalar network analyzer (SNA) and vector network analyzer (VNA) [27]. SNA can only measure the amplitude of electrical signals, while VNA can measure both the phases as well as magnitudes of the different signals. VNA can measure the complex permittivity (ε), permeability (μ) and S parameters (S_{12}, S_{21}, S_{11} and S_{22}) of EMI shielding materials. The S parameter represents the reflection and transmission coefficients of the material, and the EMI SE of the EMI shielding material can be calculated by Eqs. (3)−(7).

Based on the measurement principle of VNA, three commonly-used techniques are used to measure EMI SE:

(1) Coaxial transmission line method: The coaxial transmission line method is based on the transmission line theory and is now the preferred method for measuring the EMI SE of metallic materials. The coaxial transmission line setup comprises a VNA, a coaxial fixture and a 10 dB attenuator, as shown in Fig. 2. Tests are carried out on small doughnut-shaped samples. The signal is output through one end of the VNA, the signal is transmitted through the coaxial cable coupled with the attenuator, and finally the EMI SE of the material is obtained through the signal input at the other end. In Mg matrix materials, the coaxial transmission line method is usually used to measure the EMI SE of the sample in the frequency range of 30−1500 MHz [19,28].

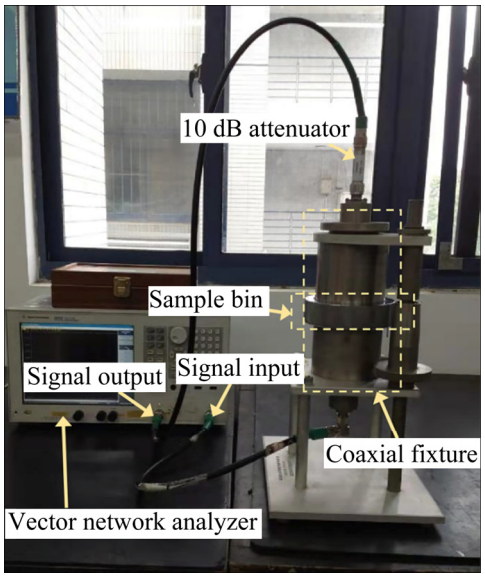

Fig. 2 Coaxial transmission line method equipment

(2) Wave guide method: The wave guide method outputs the signal through the VNA, and the signal passes through the wave guide fixture. The VNA separates the signal to obtain the corresponding *S* parameters. Figure 3 shows a diagram of two-port VNA with a wave guide fixture and the schematic diagram of signal separation. The wave guide method constrains or guides EM waves to propagate along specific geometric structures and defined routes. The ratio of the power received by the reference to the load samples gives the SE of the load material. In Mg matrix materials, the wave guide method is usually used to measure the EMI SE of the sample in the X-band (8.2−12.4 GHz) frequency range [19]. Figure 4 shows the DR-WX X-band test fixture and the corresponding VNA.

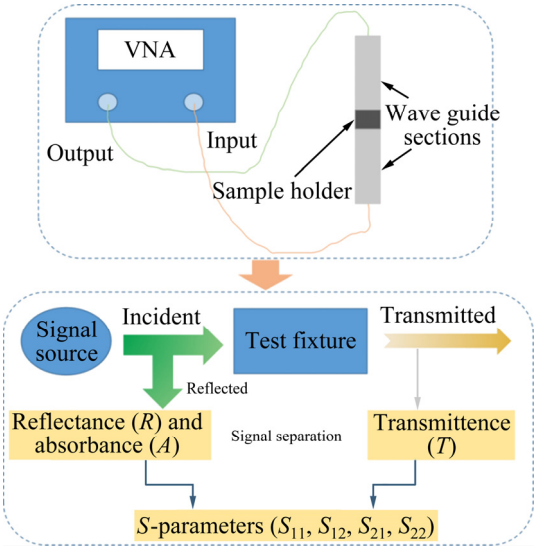

Fig. 3 Diagram of two-port VNA with wave guide fixture and schematic diagram of signal separation

(3) Free space method: It is used to evaluate the actual shielding properties of complete electronic components. It is the most realistic method for measuring the EMI SE of a material or an enclosure because it simulates the conditions that shielding materials would be subjected to during its usage. The test method involves mounting the device at a distance of 30 m from a receiving antenna and recording the radiated emissions as shown in Fig. 5 [5,19,28].

In addition to the above three methods, there are a series of EMI SE measurement methods for shielding materials such as the shielded box method, shielded room method, and the inductive electronics industry development center method. The most commonly used methods in the EMI SE measurement of Mg matrix materials are the coaxial transmission line method and wave guide method.

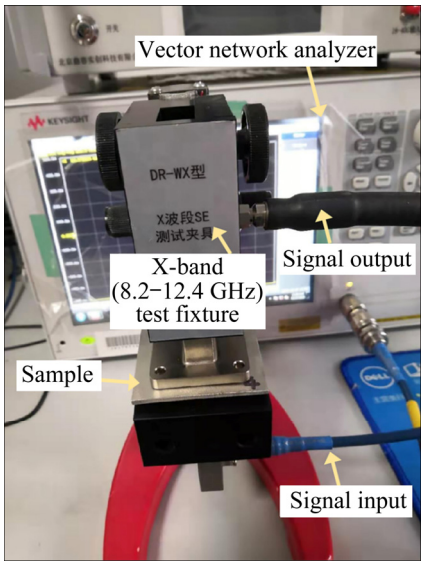

Fig. 4 DR-WX X-band test fixture and corresponding vector network analyzer (VNA)

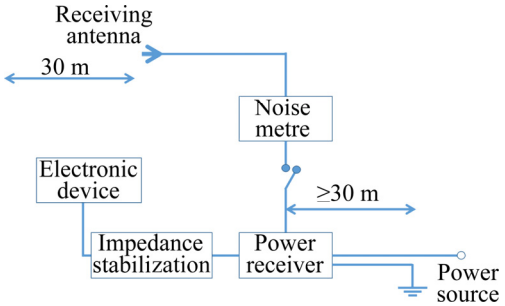

Fig. 5 Free space method SE measurement [28]

3 Mg matrix EMI shielding materials and their processes

With the widespread use of electronic equipment, the problem of radiation pollution caused by EM waves is increasing. Hence, there has been an increasing need to develop new low-cost, lightweight, EMI shielding structural materials. In this regard, Mg has proven to be the best. The source of Mg is very wide. Magnesite, magnesium-bearing dolomite, magnesium salt in salt lake area and even sea water can be used to make Mg metal. As the lightest metallic structural material for engineering applications, Mg has a density of only 1.74 g/cm^3, about 2/3 that of aluminium and 1/4 that of steel [29−32]. In addition, Mg alloy has the advantages of high specific strength and specific

stiffness, good damping property, superior electrical conductivity, excellent EMI shielding property, and easy recycling and reuse, which has attracted widespread attention in the field of EMI shielding materials [33−38]. However, pure Mg is not very good in creating an effective shield against EMI on its own. Hence, various processes are required to become suitable EMI shielding materials. Many different preparation processes are used for the fabrication of Mg matrix materials for EMI shielding. These processes include alloying, heat treatment, plastic deformation, and composite processing [39−42].

3.1 Alloying

Alloying is one of the effective methods to improve the properties of Mg alloys. Al, Zn, Li, RE (e.g. Y, Gd, Ce, Sm) and other elements are common alloying elements in Mg alloys [43−46]. The addition of alloying elements can tailor the microstructure and improve the properties of Mg alloys such as strength, plasticity, and corrosion resistance. In addition to improving these properties of Mg alloys, these alloying elements have also been found to have significant influence on the EMI shielding properties of Mg alloys. In recent years, it has been widely reported to improve the EMI shielding properties of Mg alloys through alloying methods.

Binary Mg alloy is the most fundamental alloy system in the study of Mg alloy. Zn is one of the most commonly used alloying elements in Mg alloys and plays a major role in precipitation strengthening and solid solution strengthening, which makes Mg−Zn alloys have good comprehensive mechanical properties. The maximum solid solubility of Zn in Mg is about 6.2 wt.% [47]. As the content of Zn increases, the content of the second phase in the Mg−Zn binary alloy increases, and more second phases in the alloy can precipitate during solution and subsequent aging process. The increase in the second phase content contributes to the multiple reflection loss in the alloy, but an excessive second phase leads to a decrease in the electrical conductivity of the alloy. SONG et al [48] studied the EMI SE of the Mg−xZn (x=0−5 wt.%) binary alloy in the frequency range of 30−1500 MHz and found that the Mg−4Zn in T6 state showed the best performance of EMI SE, which is 94−114 dB in the test frequency range. In addition to the influence of alloying element content, different types of alloying elements have different influences on the electrical conductivity and EMI shielding properties of Mg alloys. LUO et al [49] chose Mg−X (X=Al, Sn, Y, and Gd) binary alloys, and mainly studied the effect of different alloying elements on EMI SE of binary Mg alloys in the frequency range of 30−1500 MHz. It can be seen from Table 1 that between Al and Mg, with small volumetric difference between solute atoms and Mg atoms ($\Delta V/V_{Mg}$), small chemical valence and small number of extranuclear electron vacancies, the Mg−Al alloy exhibits the best electrical conductivity and EMI shielding properties. The $\Delta V/V_{Mg}$, the valence state of solute atoms and the configuration of extranuclear electrons may be the main reasons for the difference in electrical conductivity, and electrical conductivity is the main factor affecting the EMI shielding performance of binary magnesium alloys. Larger $\Delta V/V_{Mg}$ causes serious lattice distortion of Mg, resulting in stronger electron transmission and lattice vibration wave scattering which decreases the electrical conductivity. The higher the valence of the alloying element is, the more unfavorable the improvement of the electrical conductivity of the material is. The more the vacancies in alloying element outer orbit are, the easier the conductive electrons are absorbed, which decreases the electrical conductivity of material.

Table 1 Electrical conductivity and EMI SE values of T4 Mg−1at.%X (X=Al, Sn, Y and Gd) binary alloys and $\Delta V/V_{Mg}$, valence and configuration of extranuclear electron of four alloying elements [49]

Alloy Composition/at.%	Electrical conductivity/%(IACS)	EMI SE value/dB			$\Delta V/V_{Mg}$	Chemical valence	Configuration of extranuclear electron
		900 MHz	1200 MHz	1500 MHz			
Mg−1Al	27	80	80	80	−28.420	+3	$3s^2 3p^1$
Mg−1Sn	18	74	70	63	+16.678	+4	$4d^{10}5s^2 5p^2$
Mg−1Y	18	74	71	66	+41.732	+3	$4d^1 5s^2$
Mg−1Gd	16	70	60	59	+42.448	+2, +3	$4f^7 5d^1 6s^2$

In order to further improve the comprehensive properties of Mg alloys, ternary and above Mg alloys or composite additions of alloying elements are usually used. CHEN et al [50] prepared as-cast Mg−Y−Zr−Nd alloys with different Nd contents and studied the effect of Nd content on the EMI shielding properties of Mg−Y−Zr−Nd quaternary alloys. As shown in Fig. 6, as the Nd content increases, the $Mg_{24}Y_5$ phase content in the alloy increases, and irregular bone-like β phases precipitate on the grain boundaries when Nd content rises to 2.63 wt.%. As given in Table 2, the addition of Nd slightly reduces the relative electrical conductivity and significantly increases the size and number of phases. A large number of coarse phases enhance the multiple reflection loss of of EM waves, which can reasonably explain the fact that the SE value increases significantly at the whole testing frequency by adding Nd element. YANG et al [51] studied the EMI shielding properties of the Mg−Zn−Zr−Sm quaternary alloy and demonstrated that the increase in Sm content can consume the solid-soluted Zn atoms in the matrix of Mg to precipitate the Mg−Zn−Sm phase, resulting in an increase in electrical conductivity and the improvement of EMI shielding properties.

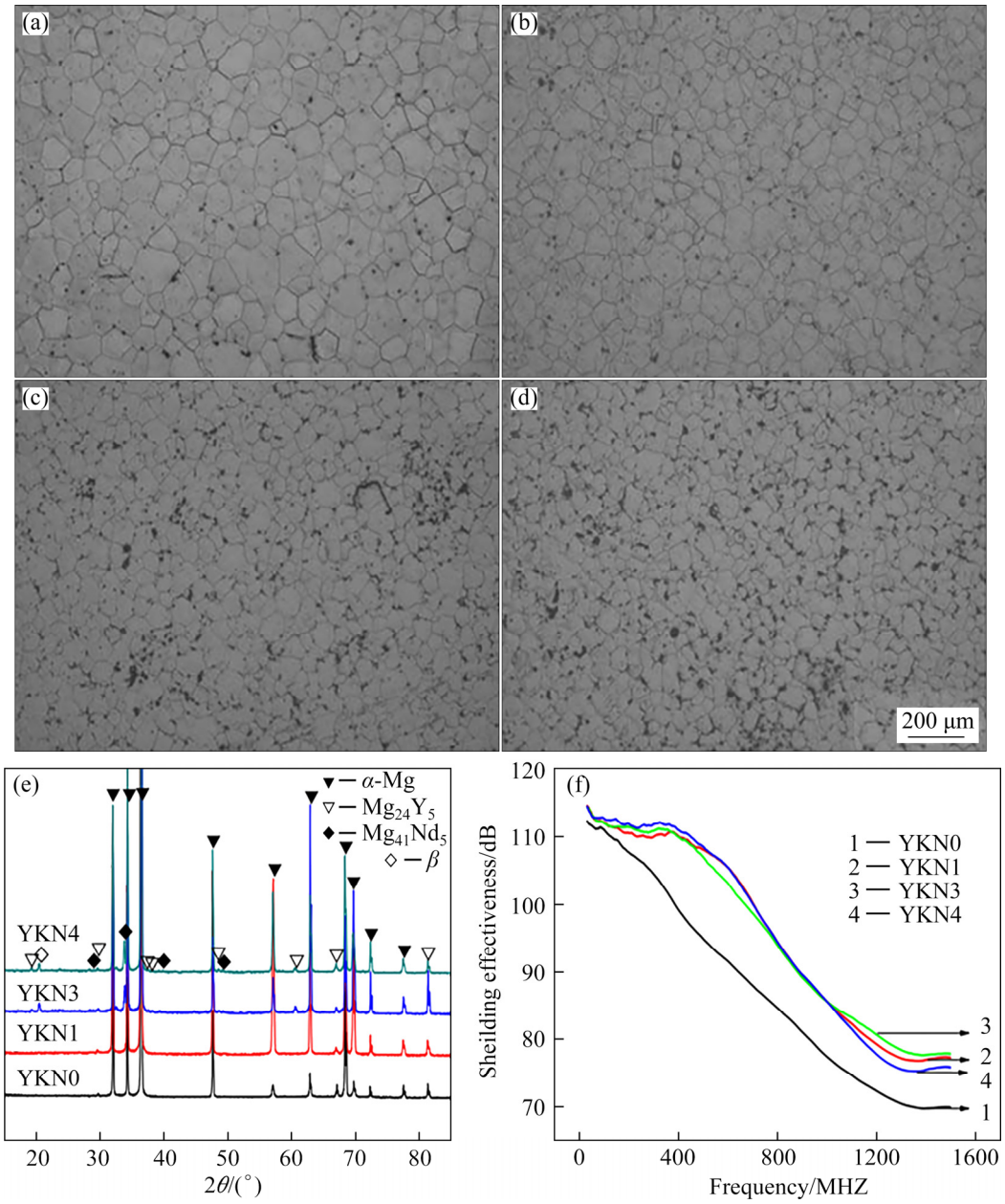

Fig. 6 Microstructures (a−d), XRD patterns (e) and EMI SE curve (f) of as-cast Mg−Y−Zr−Nd alloys with different Nd contents [50]: (a) YKN0; (b) YKN1; (c) YKN3; (d) YKN4

LIU et al [52] systematically studied the microstructure, electrical conductivity and EMI SE of the as-cast Mg−*x*Zn−*y*Y (*x*=2−5 wt.%, *y*=1−10 wt.%) alloy by composite adding Y and Zn elements. The electrical conductivity and EMI SE values of the as-cast Mg−*x*Zn−*y*Y (*x*=2−5 wt.%, *y*=1−10 wt.%) alloy are shown in Fig. 7, and the electrical conductivity and SE values of the alloy decrease with the Y/Zn ratio. Compared with Zn (+2, $3d^{10}4s^2$) element, the valence difference between Y (+3) and Mg (+2) is larger, and there are more number of vacancies in outer orbit of Y ($4d^15s^2$), which indicates that the increased Y element content more easily leads to a decrease in

Table 2 Detailed summary of properties for as-cast Mg−Y−Zr−Nd alloy [50]

Alloy	Area fraction of second phase/%	Relative conductivity/%(IACS)	SE/dB
YKN0	0	10.78±0.06	70−99
YKN1	0.062	9.39±0.05	77−109
YKN3	1.32	8.56±0.05	78−110
YKN4	1.57	8.52±0.1	75−111

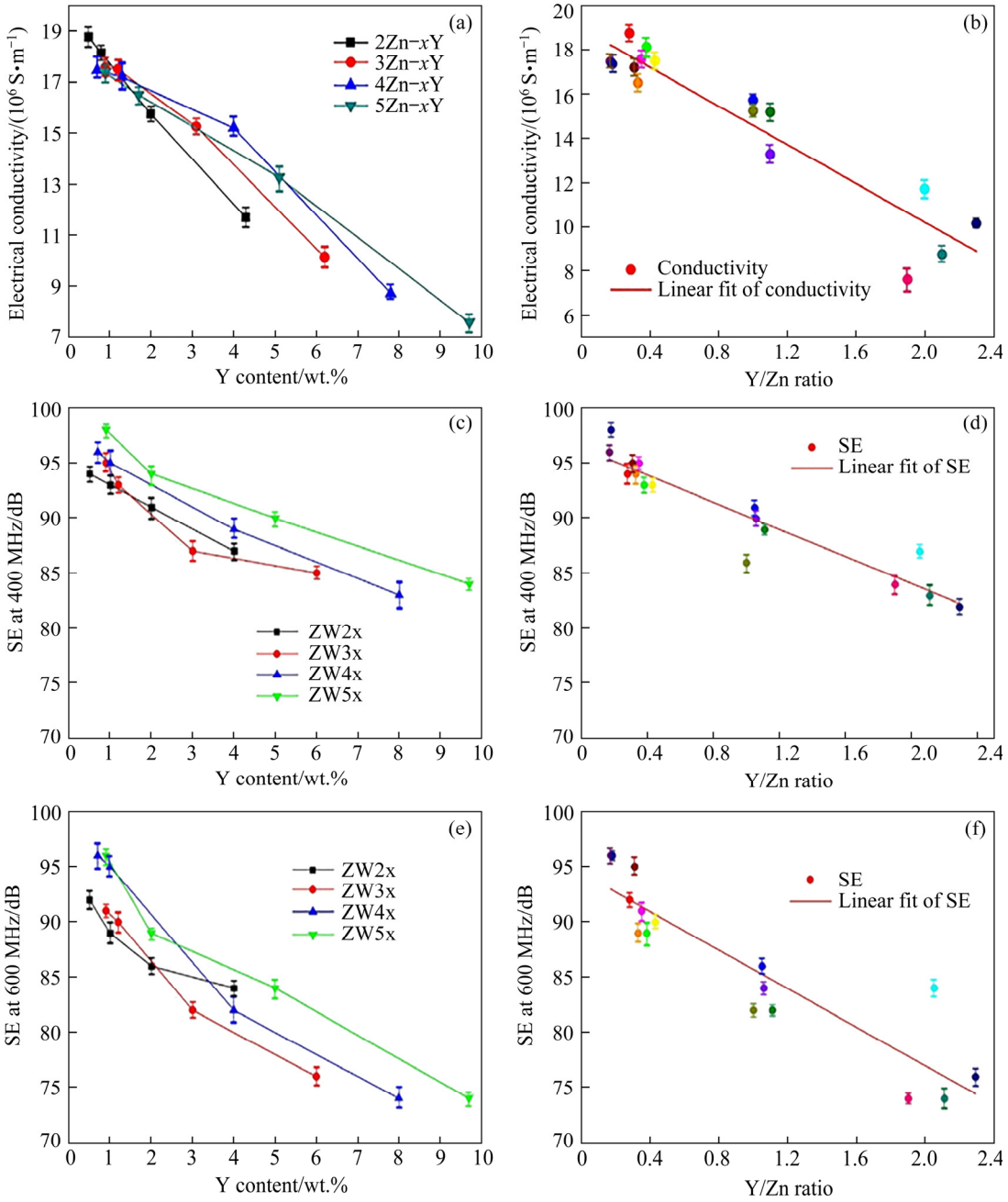

Fig. 7 Electrical conductivity of Mg−Zn−Y alloys (a); electrical conductivity variation with Y/Zn ratio (b); EMI SE of Mg−Zn−Y alloys at 400 (c) and 600 MHz (e); EMI SE variation with Y/Zn ratio at 400 (d) and 600 MHz (f) [52]

electrical conductivity and EMI SE. In addition, more second phases and the formation of semicontinuous network structure can improve the SE value at high frequencies (600 MHz, 96 dB) when Y content is low in the alloys containing more Zn (ZW51 alloy).

In a word, the main reason for improving the EMI shielding properties of Mg matrix materials through alloying is that alloying elements cause more second phases. The precipitation of the second phase can not only consume the solid-soluted atoms in the matrix and improve the overall electrical conductivity of the alloy, but also cause more multiple reflection losses due to the difference in impedance between the second phase and the matrix. Excellent electrical conductivity and more multiple reflection loss of EM waves are important factors for Mg matrix materials to obtain high EMI SE. It is worth noting that the selection of alloying elements is also very important. Valence of alloying elements, configuration of extranuclear electron and volumetric difference are main reasons for the variations in the electrical conductivity. Therefore, in the selection of alloying elements, it should be chosen to have smaller $\Delta V/V_{Mg}$ and smaller valence difference with Mg, and there are fewer vacancies in its own outer orbit. At present, more reasonable alloying elements are selected and the synergistic effect of multiple alloying elements is used to maximize the electrical conductivity of Mg matrix materials to achieve efficient shielding of EM waves.

3.2 Heat treatment

Heat treatment can be used to control the microstructure and properties of Mg alloys and give full play to their potential. The common heat treatment methods in Mg alloys include solution treatment (T4), homogenization treatment and aging treatment (T5, T6), etc [53−56]. If the heat treatment can make the solid-soluted atoms precipitate from the matrix by the formation of the second phase, or eliminate the defects in the alloy, its EMI shielding properties can be improved. In addition, the optimization of the heat treatment process to control the morphology, size and quantity of the second phase and the orientation relationship between the second phase and matrix is of great significance to improve the EMI shielding properties of the Mg alloy.

CHEN et al [57−59] systematically investigated the EMI shielding properties of extruded ZK60 alloy with different heat treatment processes. After T4 and T6 treatment, the EMI shielding properties of the extruded ZK60 alloy are significantly improved. After T4 treatment, most of second phases are dissolved, causing the supersaturated solid solution of matrix. Subsequent aging results in the precipitation of fine second phases. The precipitation of the second phase not only increases the number of effective reflection interfaces for EM waves, but also reduces the number of alloying elements in the solid solution. The resistivity contribution for alloying elements in solid solution is an order of magnitude higher than the resistivity of the alloying elements in the form of second phases [57]. Therefore, the decrease in the number of alloying elements in the solid solution contributes to the increase of the electrical conductivity, which leads to the increase of EMI SE. With the increase of aging time, the number of precipitates increases and the size of precipitates is also changed. In addition to the number of phases affecting EMI SE of the alloy, the size of the phase is also an important factor. The excessive coarsening of the precipitates results in the reduced density of phase interfaces between the precipitated phase and matrix, which leads to a decrease in the multiple reflection loss of EM waves. We have also drew a similar conclusion in the heat treatment experiment of Mg−8Li−6Y−2Zn alloy [60]. We proved that the dendritic coarse $(Mg,Zn)_{24}Y_5$ phase precipitating along the grain boundary in the as-cast alloy by heat treatment transforms into a long strip LPSO phase and many small granular $(Mg,Zn)_{24}Y_5$ phases diffuse, which greatly improves the EMI SE of the alloy.

GAO et al [61] controlled the grain orientation of binary Mg alloys by rolling deformation, and controlled the precipitation of the second phase along specific crystal planes through subsequent aging treatment, so as to obtain Mg alloys with high EMI shielding properties. As shown in Fig. 8(a), after aging treatment of as-rolled Mg−Zn alloy and Mg−Sn alloy, rod-like $MgZn_2$ phase precipitates along the $(11\bar{2}0)$ plane of Mg−Zn alloy, while plate-like Mg_2Sn phase precipitates along (0001) basal plane of Mg−Sn alloy. According to the double-layer shield model, as shown in Fig. 8(b), the plate-like Mg_2Sn precipitating on the (0001)

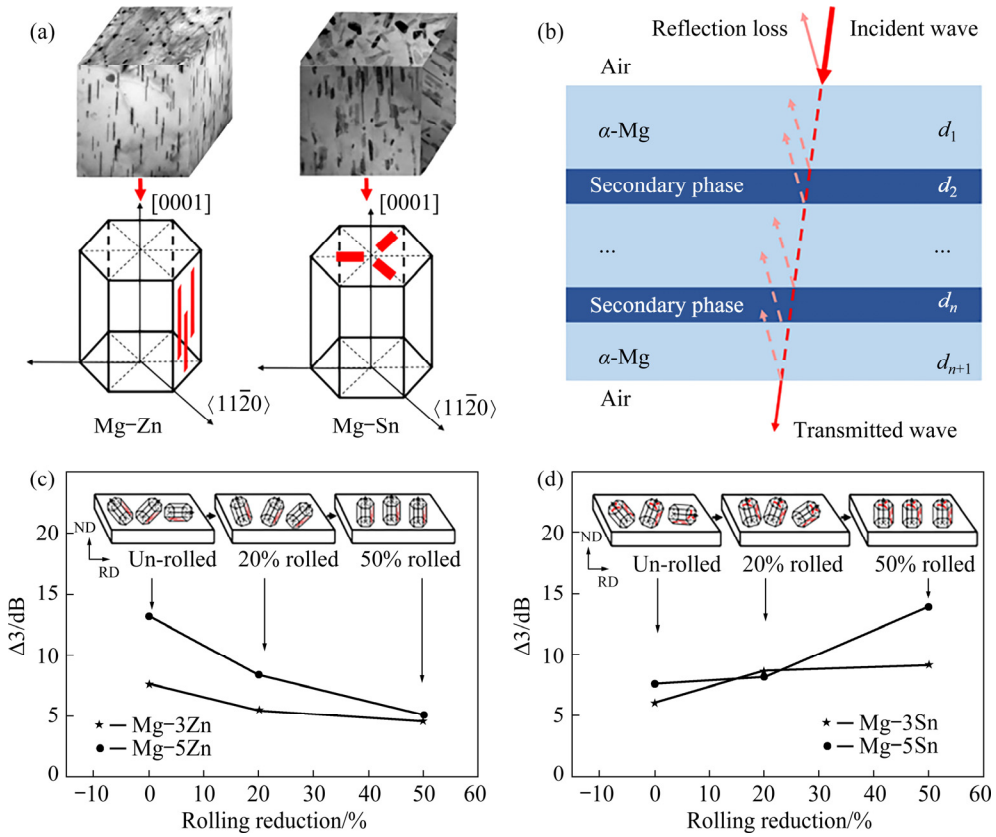

Fig. 8 Schematic of Mg−Zn and Mg−Sn orientation (a); double-layer shield model (b); effect of secondary-phase orientation on EMI shielding properties of Mg−Zn (c) and Mg−Sn (d) alloys ($\Delta3=SE_{aged\ (60\ h)}-SE_{solutionized}$) [61]

basal plane has a larger EM waves contact area than the rod-like $MgZn_2$ phase precipitating along the (11$\bar{2}$0) plane, which is more conducive to improving EMI SE. Therefore, in the Mg alloy with large rolling strain, the alloy obtains a larger amount of the second phase precipitating along (0001) basal plane through aging treatment, which helps to improve EMI SE, as shown in Figs. 8(c, d).

Based on the above discussion, the heat treatment process and alloying method are essentially similar for improving the EMI SE of Mg matrix materials. The same is that both more solid-soluted atoms in the matrix are consumed by precipitaton of the second phase to improve the electrical conductivity. The difference is that the morphology and size of the second phase and its orientation relationship with the matrix can be adjusted by optimizing the heat treatment process, so as to obtain more reflection interfaces of EM waves. Therefore, the EMI shielding properties of Mg matrix materials can be effectively improved through reasonable alloying design in the early stage and optimization of subsequent heat treatment process.

3.3 Plastic deformation

As-cast Mg alloys have poor comprehensive properties due to structural defects such as loose inclusions. Plastic deformation can effectively improve the microstructure and comprehensive properties of Mg alloys. However, Mg crystal with hexagonal close packed (HCP) structure has only three slip systems at room temperature, and its plastic deformation ability is lower than that of face-centered cubic (FCC) and body-centered cubic (BCC) metals. At present, the plastic deformation methods of Mg alloys mainly include rolling, extrusion, severe plastic deformation (SPD), etc. These plastic deformation processes mainly use external forces to change the grain orientation, the morphology and distribution of precipitated phases, and eliminate internal defects of alloy [62−67]. The EMI shielding property of Mg alloys is also changed accordingly.

Rolling is an effective plastic deformation method that can change the grain size and grain orientation of the alloy. Mg alloy is easy to form (0002) basal texture during rolling process. SONG et al [68] studied the effect of texture on the EMI

shielding properties of AZ31 alloys by different rolling strains. As shown in Figs. 9(a−d), as the rolling strain increases, the grains of AZ31 alloy are gradually refined, and the (0002) basal texture intensity gradually increases. This means that there are more grains and their *c*-axis gradually aligns close to the ND direction of as-rolled samples. As the rolling strain increases, the EMI SE of the AZ31

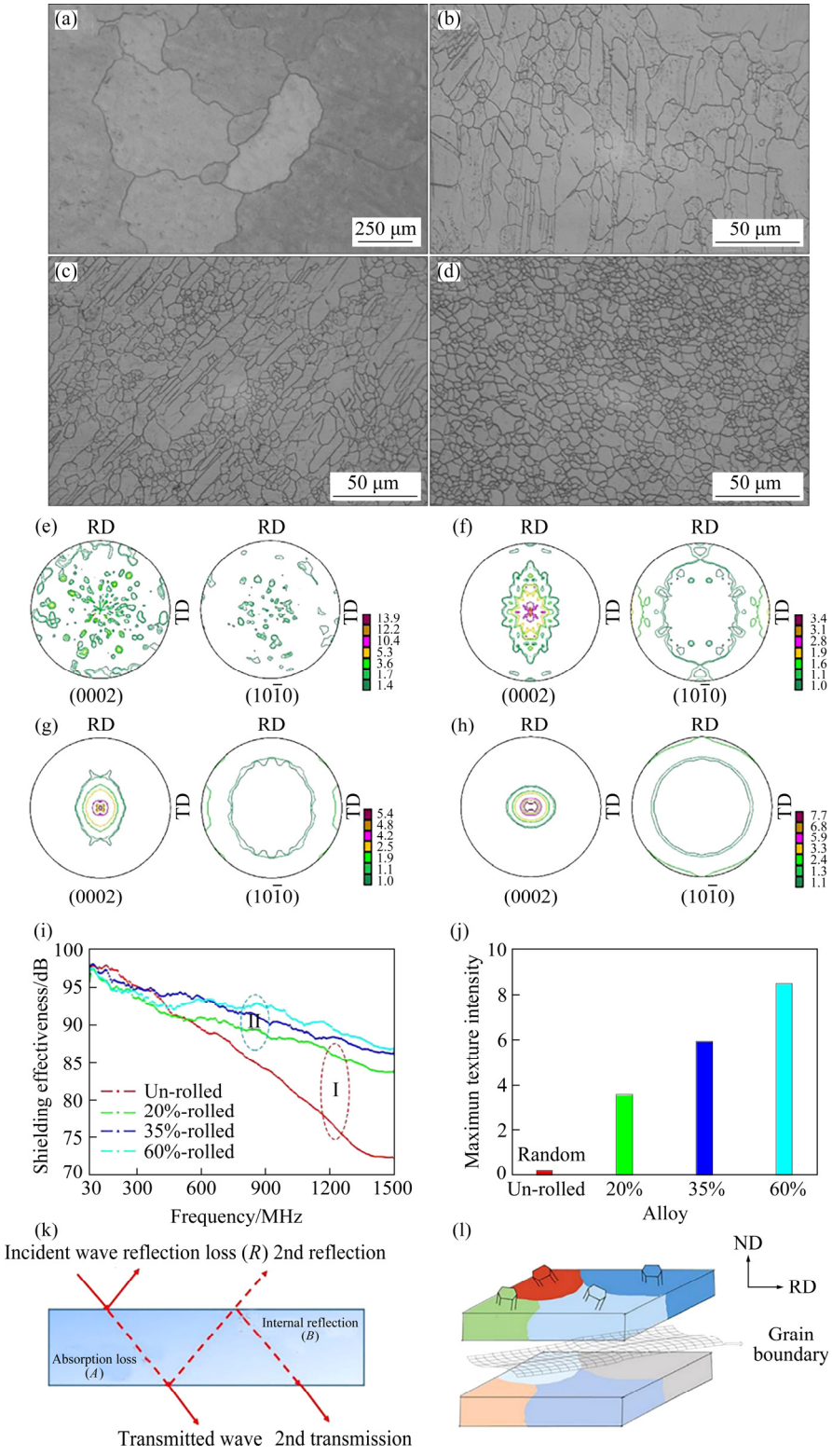

Fig. 9 Optical microstructures and pole figures of AZ31 alloys ((a, e) Un-rolled, (b, f) 20% rolled, (c, g) 35% rolled, (d, h) 60% rolled); EMI SE of investigated AZ31 alloys in 30−1500 MHz range (i); maximum texture intensity of un-rolled, 20% and 35%, 60% rolled AZ31 alloys (j); mechanism of EMI shielding (k); schematic representation of grain orientation and microstructure of alloy (l) [68]

alloy increases, as shown in Fig. 9(e). The movement of free electrons along the *c*-axis of grain has a larger mean free path. Thus, the enhancement of (0002) basal texture intensity increases the electrical conductivity of the as-rolled sheet surface, thus expanding the impedance mismatch between air and sample and improving SE_R and SE_T, as shown in Figs. 9(f−h). Generally, the addition of Li element can convert the crystal structure of Mg from HCP to BCC, which greatly improves the formability of Mg alloys [69]. The addition of 5.7−10.3 wt.% Li element in Mg to form a Mg−Li alloy with α-Mg (HCP) + β-Li (BCC) dual-phase structure [70], in which the α-Mg + β-Li dual-phase interface has a certain positive effect on EM waves reflection. For Mg−Li alloys with α-Mg + β-Li dual-phase structure, in addition to changing the grain orientation in the alloy, the rolling stress also makes the α/β duplex phase alternately arranged along the RD direction of the alloy, as shown in Fig. 10, increasing SE_A and SE_M [71].

During extrusion process, Mg alloy is subjected to strong three-dimensional compressive stress state, which can effectively refine the grains of the Mg alloy, the structure becomes denser, and the defects are reduced. XIAO et al [72] studied the EMI shielding properties of Mg−13Gd−4Y−2Zn−0.5Zr alloys with different extrusion strains. It is found that the grains of Mg alloy with large extrusion strain are refined and the grain boundary area is increased, which significantly improves the EMI shielding properties of the alloy in high frequency band. In addition, the massive extrusion strain also changes the morphological distribution of the second phase in the Mg alloy. CHEN et al [73] found that the MgZnCu phases distributing in a network-like along the grain boundary in the as-cast Mg−Zn−2.32Cu−Zr alloy are affected by the extrusion stress, move away from grain boundaries and are destroyed into smaller particles during the hot extrusion, as shown in Fig. 11, which effectively increases the number of reflected interfaces of EM waves.

The SPD technology can manufacture nano-crystalline and ultrafine grains through large plastic deformation, thereby improving the strength and toughness of the material [74]. As one of the common SPDs, accumulative roll bonding (ARB) technology has been widely used to prepare various high strength and toughness metallic materials with

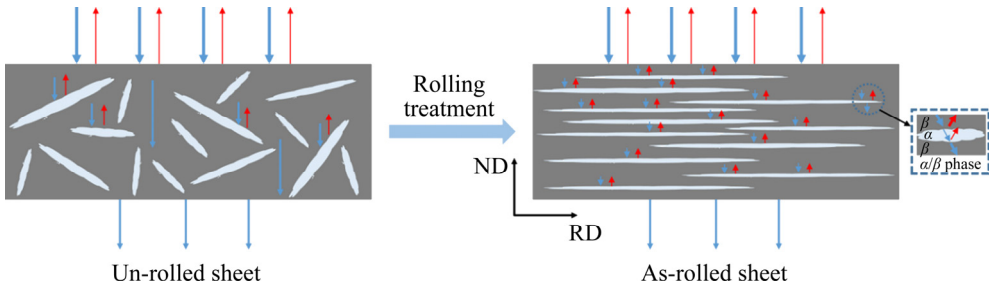

Fig. 10 EMI shielding model for RD−ND plane of un-rolled and as-rolled sheets

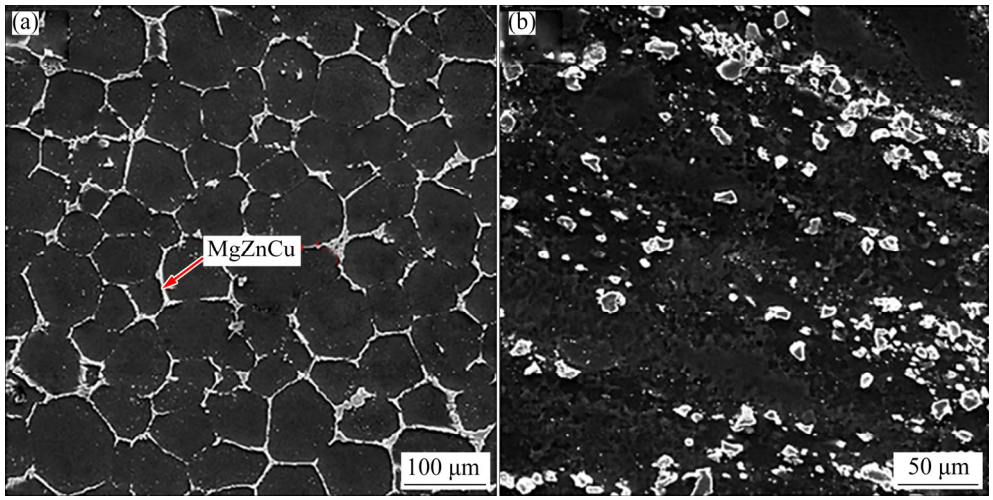

Fig. 11 SEM micrographs of Mg−Zn−2.32Cu−Zr alloy [73]: (a) As-cast; (b) Extruded

ultrafine grains [56,75−78]. However, the research on ARB technology is currently focused on improving mechanical properties such as strength and elongation of sheets, and there are relatively few researches on functional aspects such as EMI shielding properties. In our previous research, the EMI shielding properties of Mg−9Li−3Al−1Zn alloy processed by ARB were studied in detail to further expand the application of ARBed Mg−Li alloy [79]. The results show that the α-Mg + β-Li dual-phase interface, texture, second phases and ARB roll-bonding interface in the ARBed Mg−9Li−3Al−1Zn alloy have significant influence on the EMI shielding properties. ARB processing produced a roll-bonding interface between Mg−Li plates, and the number of roll-bonding interfaces increased exponentially as the ARB passes increased. According to the impedance mismatch theory, the increase of the roll-bonding interface facilitates the absorption loss and multiple reflection loss of the EM waves in the sheet, as shown in Fig. 12(a). Therefore, the comprehensive action of the α-Mg + β-Li dual-phase interface, texture, second phases and ARB roll-bonding interface, as shown in Fig. 12(b), significantly improves the EMI SE of the Mg−Li sheet. Figure 12(c) shows that the SE value of ARB3 sheet is 96−107 dB in the frequency range of 30−1500 MHz.

In general, regardless of which deformation process is adopted, the essence of improving the EMI shielding properties of Mg matrix materials is to enhancement of (0002) basal texture intensity and obtain more interfaces (α/β dual-phase interface, second phase interface and roll-bonding interface), thus increasing the reflection loss and absorption loss of the EM waves.

3.4 Composite processing

The addition of reinforcements to prepare high-performance Mg matrix composites is one of the effective measures to improve the comprehensive properties of Mg alloys such as strength, plasticity, corrosion resistance, and EMI shielding properties [42]. Mg matrix composites have the conventional characteristics of Mg alloys, and can realize comprehensive properties regulation of materials as well as breaking through the mechanical and functional properties that single components do not have [80−83]. At present, the composite processing technology of Mg matrix composites mainly includes ARB, friction stir welding, and powder metallurgy [83−87]. In order to improve the EMI shielding properties of Mg matrix materials, the reinforcements used mainly include other metallic materials, ferrites, carbon materials (carbon nanotubes, carbon fibers, etc).

In recent years, the significant progress has been made in studying the EMI shielding properties of Mg matrix composites. LU et al [88] used the raw fly ash cenospheres (FACs) and FACs modified by $Ca(OH)_2$ (M-FACs) as the reinforcements to prepare two kinds of AZ91 composites by melt stirring. Figure 13 shows the microstructure, EMI

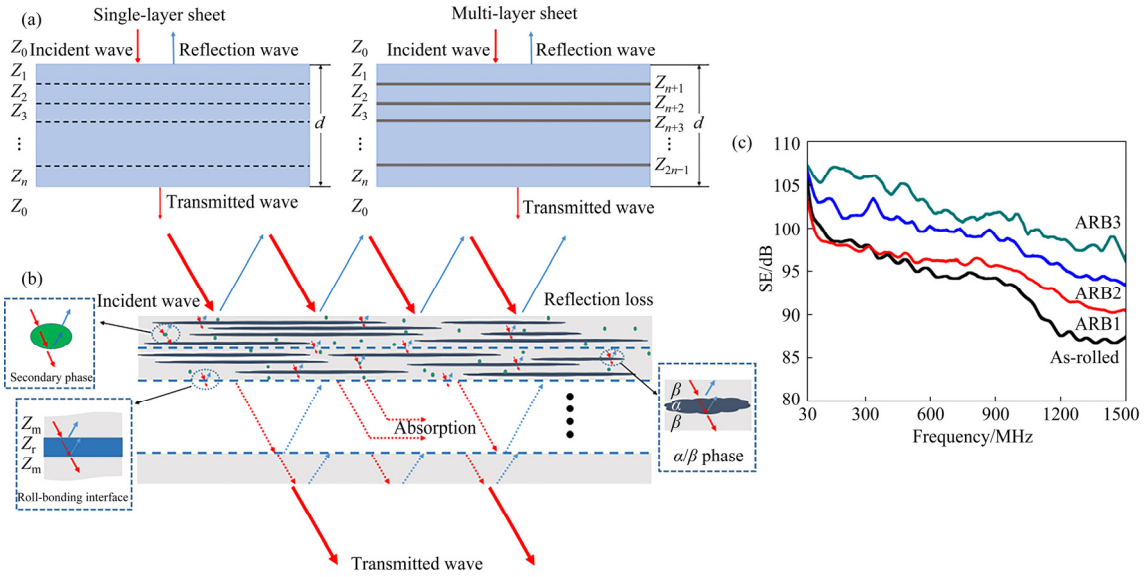

Fig. 12 Ideal model of multi-layer shielding materials prepared by ARB (a); multilayer interface electromagnetic shielding mechanism (b); EMI shielding properties of ARB alloys in 30−1500 MHz range (c) [79]

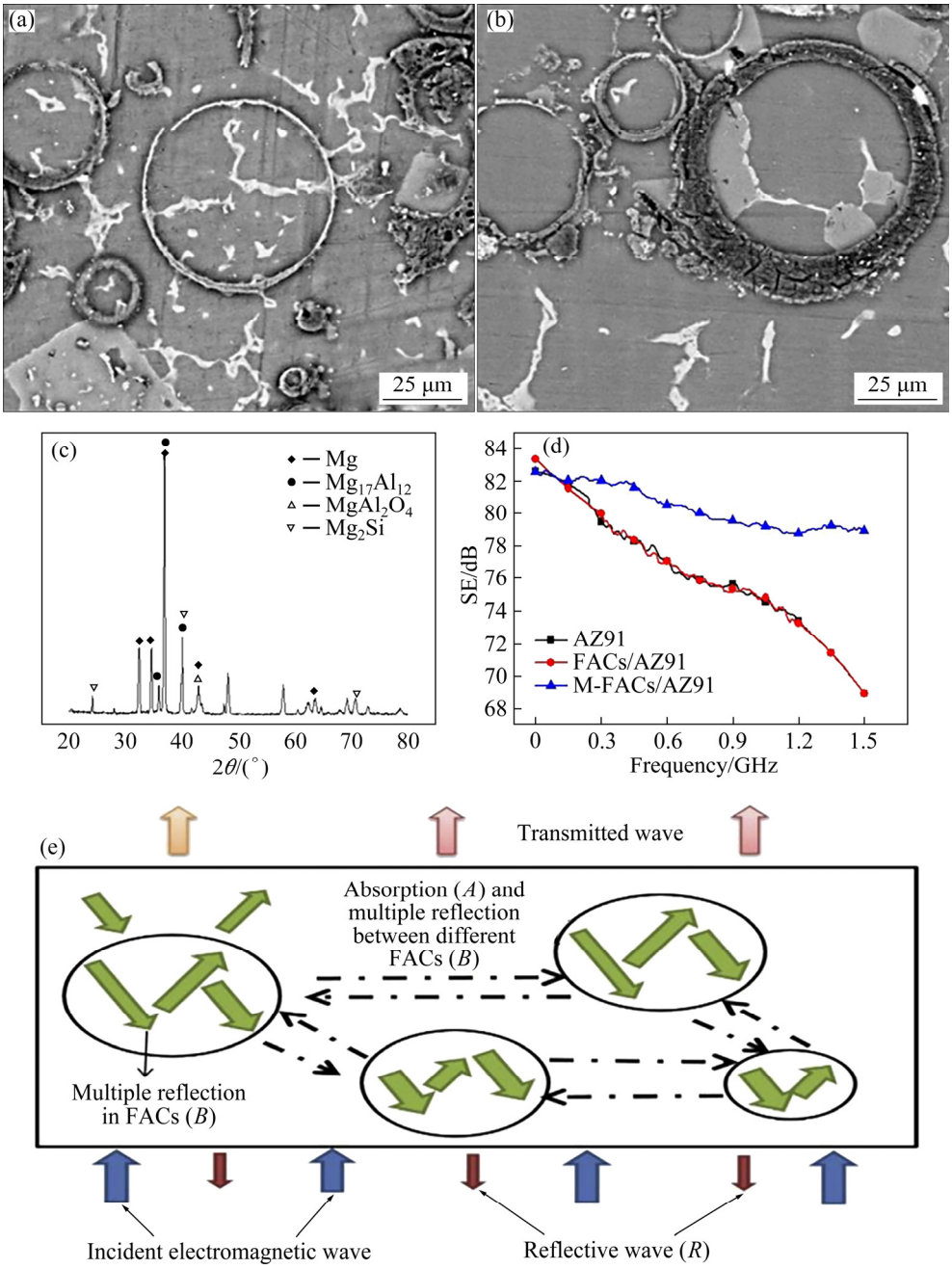

Fig. 13 SEM image of two kinds of composites ((a) FACs/AZ91, (b) M-FACs/AZ91); XRD result of FACs/AZ91 composite (c); EMI SE properties of alloy and composites (d); mechanism of SE property (e) [88]

SE curve and corresponding EMI shielding mechanism of the composites. Most of the unmodified FACs were severely broken in the composites, but most of the FACs kept completely integrated in the composites reinforced by modified FACs, which is exactly why M-FACs/AZ91 has more excellent EMI SE (72.9−82.5 dB). The existence of FACs with completely hollow structure leads to the absorption of the EM waves as well as the multiple reflection between different FACs. PANDEY et al [89,90] used the disintegrated melt deposited (DMD) process to prepare Mg−Fe and Mg−Ti composites, and studied the influence of difference in reinforcement and content on the X-band (8.2−12.4 GHz) EMI shielding properties of Mg matrix composites. By introducing insoluble particles into Mg matrix, the increase of porosity in the composite is used to improve the absorption loss of EM waves. Furthermore, the Mg−Fe composite is transformed into a ferromagnetic material by introducing ferromagnetic Fe particles into the paramagnetic Mg matrix, which increases

the absorption efficiency of EM waves of the composite.

Inspired by the ideas mentioned above, our group reported unique multi-layer structure Mg−9Li matrix composite composed of seven layers for effectively shielding EM waves [91]. The composite was prepared by a multi-layer composite rolling process, as shown in Fig. 14. In the composite, Mg−9Li alloy served as the reflective layer, and $Ni_{0.4}Zn_{0.4}Co_{0.2}Fe_2O_4$ (NZCF) particles synthesized by sol−gel autoignition method served as the absorption layer. The optimal combination of magnetic fillers along with metal material achieved the high efficiency of reflection and absorption of EM waves. In another report [92], we prepared Mg−9Li−3Zn−0.5Gd/MWCNTs composite with high electrical conductivity and EMI shielding properties through combined process of heat treatment + electrophoretic deposition (EPD) + ARB. The uniform dispersion of MWCNTs and multi-pass ARB process make many fine phases precipitate in Mg−9Li−3Zn−0.5Gd sheets, which greatly increases the electrical conductivity of the composite, and enables the composite to achieve over 99% reflection of the EM waves.

To sum up, the key to improve the EMI shielding performance of Mg matrix materials by the composite processing method is the selection of reinforcement type and amount. For highly electrical conductivity and paramagnetic Mg matrix materials, different types of reinforcements, such as magnetic medium and dielectric, are added to the inside or surface of the matrix to improve the EMI shielding properties. Besides, it is particularly

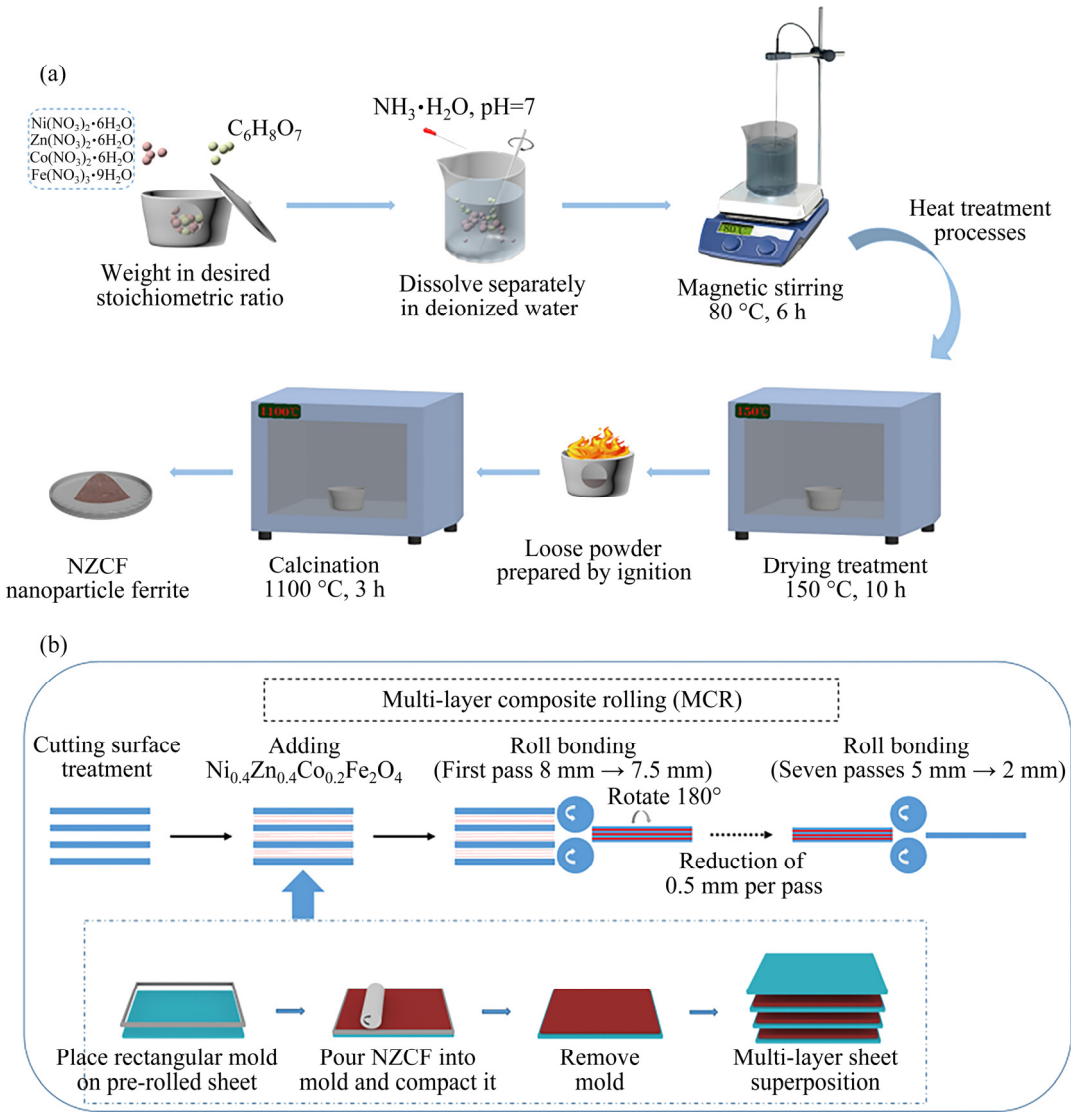

Fig. 14 Schematic diagram of NZCF ferrite preparation process (a), and preparation procedure for Mg−9Li/NZCF composites (b) [91]

important to select the appropriate preparation process. Through SPD and other processing processes, in addition to making the reinforcement evenly dispersed in the matrix, the microstructure of Mg matrix materials can be effectively improved and the EM wave reflection interface is increased, resulting in the increase of the reflection loss and absorption loss of EM waves.

4 Conclusions and outlook

At present, the low cost, lightweight, high strength, easy processibility, and good recyclability of Mg matrix materials have received great popularity for EM wave shielding. This review summarizes the main features, preparation methods, the latest research progress and shielding mechanism of Mg matrix EMI shielding materials. The key to improve the EMI shielding properties of Mg matrix materials is to improve the electrical conductivity. In addition, the increase in the number of interfaces (α/β dual-phase interface, second phase interface, roll-bonding interface, particulate reinforcement interface) within the material is also beneficial to the absorption loss and multiple reflection loss of EM waves in the material. Therefore, increasing the electrical conductivity as much as possible and having more interfaces simultaneously are the keys to achieve high EMI shielding properties of Mg matrix materials. To obtain the high electrical conductivity and multi-interface, the strategies can be found from the aspects of the selection of alloying element, the optimization of heat treatment, the plastic deformation, and the addition of reinforcements.

(1) In the selection of alloying elements, the favorable alloying elements should have smaller $\Delta V/V_{Mg}$ and smaller valence difference with Mg, and fewer vacancies in their own outer orbit. In addition, too many alloying elements lead to an increase in the content of solid-soluted atoms, which is not conducive to the improvement of the electrical conductivity of the material.

(2) The purpose of the heat treatment process is to consume as much as possible solid-soluted atoms in the matrix by precipitation of the second phase to improve the electrical conductivity. The morphology and size of the second phase and its orientation relationship with the matrix can also be tailored by optimizing the heat treatment process, so as to obtain more favorable EM wave reflection interfaces.

(3) Through the plastic deformation process, the basal texture of the alloy is strengthened, the microstructure is improved, and the morphology and size of the second phase and its orientation relationship with the matrix conducive to EM wave reflection are obtained.

(4) By adding reinforcements with different features, the electrical and magnetic properties of Mg matrix materials can be improved, thereby increasing the reflection and absorption loss of EM waves.

The development of Mg matrix EMI shielding materials is a complex process. The current research only stays in the aspect of laboratory basic research, and there is still a long way to go before the engineering application.

Based on engineering applications of Mg matrix materials, not only EMI shielding properties should be considered, but also necessary properties such as corrosion resistance and mechanical properties as structural materials should be possessed. In addition, cost issues (such as the addition of expensive alloying elements and excessive addition) are also important to be considered. Therefore, the development of low-cost Mg matrix EMI shielding materials with excellent comprehensive performance is one of the key research directions in the future. With the continuous advancement of science and technology, the research system, preparation method and comprehensive performance of Mg matrix EMI shielding materials will continue to be improved.

Acknowledgments

This work was supported by the National Natural Science Foundation of China (Nos. 51871068, 51771060, 51971071, 52011530025), Domain Foundation of Equipment Advance Research of 13th Five-year Plan, China (No. 61409220118), the Fundamental Research Funds for the Central Universities, China (No. 3072020CFT1006), the Fundamental Research Funds for the Heilongjiang Universities, China (No. 2020-KYYWF-0532), PhD Student Research and Innovation Fund of the Fundamental Research Funds for the Central Universities, China (No.

3072021GIP1002), and Zhejiang Province Key Research and Development Plan, China (No. 2021C01086).

References

[1] LIU Pei-jiang, YAO Zheng-jun, VINCENT M H N, ZHOU Jin-tang, YANG Zhi-hong, KONG Ling-bing. Enhanced microwave absorption properties of double-layer absorbers based on spherical NiO and $Co_{0.2}Ni_{0.4}Zn_{0.4}Fe_2O_4$ ferrite composites [J]. Acta Metallurgica Sinica (English Letters), 2018, 31: 171−179. doi: 10.1007/s40195-017-0612-5.

[2] WANASINGHE D, ASLANI F, MA Guo-wei. Electromagnetic shielding properties of carbon fibre reinforced cementitious composites [J]. Construction and Building Materials, 2020, 260: 120439. doi: 10.1016/j.conbuildmat.2020.120439.

[3] GUO Hong-tao, CHEN Yi-ming, LI Yang, ZHOU Wei, XU Wen-hui, PANG Liang, FAN Xiao-meng, JIANG Shao-hua. Electrospun fibrous materials and their applications for electromagnetic interference shielding: A review [J]. Composites Part A: Applied Science and Manufacturing, 2021, 143: 106309. doi: 10.1016/j.compositesa.2021.106309.

[4] LIU He-guang, WU Shao-qing, YOU Cai-yin, TIAN Na, LI Yuan, CHOPRA N. Recent progress in morphological engineering of carbon materials for electromagnetic interference shielding [J]. Carbon, 2021, 172: 569−596. doi: 10.1016/j.carbon.2020.10.067.

[5] WANASINGHE D, ASLANI F. A review on recent advancement of electromagnetic interference shielding novel metallic materials and processes [J]. Composites Part B: Engineering, 2019, 176: 107207. doi: 10.1016/j.compositesb.2019.107207.

[6] JANG J M, LEE H S, SINGH J K. Electromagnetic shielding performance of different metallic coatings deposited by arc thermal spray process [J]. Materials, 2020, 13(24): 1−15. doi: 10.3390/ma13245776.

[7] GUPTA S, TAI Nyan-hwa. Carbon, materials and their composites for electromagnetic interference shielding effectiveness in X-band [J]. Carbon, 2019, 152: 159−187. doi: 10.1016/j.carbon.2019.06.002.

[8] SAWAI P, CHATTOPADHAYA P P, BANERJEE S. Synthesized reduce graphene oxide (rGO) filled polyetherimide based nanocomposites for EMI shielding applications [J]. Materials Today: Proceedings, 2018, 5(3): 9989−9999. doi: 10.1016/j.matpr.2017.10.197.

[9] CHOI Y S, YOO Y H, KIM J G, KIM S H. A comparison of the corrosion resistance of Cu−Ni−stainless steel multilayers used for EMI shielding [J]. Surface and Coatings Technology, 2006, 201(6): 3775−3782. doi: 10.1016/j.surfcoat.2006.03.040.

[10] HUANG Chi-yuan, MO Wen-wei, ROAN Ming-lih. Studies on the influence of double-layer electroless metal deposition on the electromagnetic interference shielding effectiveness of carbon fiber/ABS composites [J]. Surface and Coatings Technology, 2004, 184(2/3): 163−169. doi: 10.1016/j.surfcoat.2003.11.010.

[11] HOU Lei, BI Si-yi, ZHAO Hang, XU Yu-meng, MU Yu-hang, LU Yin-xiang. Electroless plating Cu−Co−P polyalloy on UV/ozonolysis irradiated polyethylene terephthalate film and its corrosion resistance [J]. Applied Surface Science, 2017, 403: 248−259. doi: 10.1016/j.apsusc.2017.01.182.

[12] BHOSALE S D, GAIKWAD S D, GADVE R D, GOYAL R K. Synergistic effects of graphene nanoplatelets on X-band electromagnetic interference shielding, thermal expansion and thermal stability of poly(ether-ketone) based nanocomposites [J]. Materials Science and Engineering B, 2021, 265: 115038. doi: 10.1016/j.mseb.2020.115038.

[13] KITTUR J, DESAI B, CHAUDHARI R, LOHARKAR P K. A comparative study of EMI shielding effectiveness of metals, metal coatings and carbon-based materials [J]. IOP Conference Series: Materials Science and Engineering, 2020, 810: 012019. doi: 10.1088/1757-899X/810/1/012019.

[14] KRUŽELÁK J, KVASNIČÁKOVÁ A, HLOŽEKOVÁ K, HUDEC I. Progress in polymers and polymer composites used as efficient materials for EMI shielding [J]. Nanoscale Advances, 2021, 3(1): 123−172. doi: 10.1039/D0NA00760A.

[15] ZHANG Ji-jun, WANG Ze-xuan, LI Jia-wei, DONG Ya-qiang, HE Ai-na, TAN Guo-guo, MAN Qi-kui, SHEN Bin, WANG Jun-qiang, XIA Wei-xing, SHEN Jun, WANG Xin-min. Magnetic-electric composite coating with oriented segregated structure for enhanced electromagnetic shielding [J]. Journal of Materials Science & Technology, 2022, 96: 11−20. doi: 10.1016/j.jmst.2021.05.001.

[16] YANG Yan, XIONG Xiao-ming, JING Chen, PENG Xiao-dong, CHEN Dao-lun, PAN Fu-sheng. Research advances in magnesium and magnesium alloys worldwide in 2020 [J]. Journal of Magnesium and Alloys, 2021, 9(3): 705−747. doi: 10.1016/j.jma.2021.04.001.

[17] WANG Qing-hang, JIANG Bin, CHEN Dao-lun, JIN Zhao-yang, ZHAO Ling-yu, YANG Qing-shan, HUANG Guang-sheng, PAN Fu-sheng. Strategies for enhancing the room-temperature stretch formability of magnesium alloy sheets: A review [J]. Journal of Materials Science, 2021, 56: 12965−12998. doi: 10.1007/s10853-021-06067-x.

[18] LI Ming-yao, GUPTA S, CHANG Ching, TAI Nyan-hwa. Layered hybrid composites using multi-walled carbon nanotube film as reflection layer and multi-walled carbon nanotubes/neodymium magnet/epoxy as absorption layer perform selective electromagnetic interference shielding [J]. Composites Part B: Engineering, 2019, 161: 617−626. doi: 10.1016/j.compositesb.2018.12.130.

[19] SANKARAN S, DESHMUKH K, AHAMED M B, KHADHEER PASHA S K. Recent advances in electromagnetic interference shielding properties of metal and carbon filler reinforced flexible polymer composites: A review [J]. Composites Part A: Applied Science and Manufacturing, 2018, 114: 49−71. doi: 10.1016/j.compositesa.2018.08.006.

[20] ZHANG Guo-zhu, QIN Shu-yang, YAN Long-ge, ZHANG Xin-fang. Simultaneous improvement of electromagnetic shielding effectiveness and corrosion resistance in magnesium alloys by electropulsing [J]. Materials Characterization, 2021, 174: 111042. doi: 10.1016/j.matchar.2021.111042.

[21] GANGULY S, BHAWAL P, RAVINDREN R, DAS N C. Polymer nanocomposites for electromagnetic interference shielding: A review [J]. Journal of Nanoscience and Nanotechnology, 2018, 18(11): 7641−7669. doi: 10.1166/jnn.2018.15828.

[22] KWON S, MA R, KIM U, CHOI H R, BAIK S. Flexible electromagnetic interference shields made of silver flakes, carbon nanotubes and nitrile butadiene rubber [J]. Carbon, 2014, 68: 118−124. doi: 10.1016/j.carbon.2013.10.070.

[23] HONG Y K, LEE C Y, JEONG C K, LEE D E, KIM K, JOO J. Method and apparatus to measure electromagnetic interference shielding efficiency and its shielding characteristics in broadband frequency ranges [J]. Review of Scientific Instruments, 2003, 74(2): 1098−1102. doi: 10.1063/1.1532540.

[24] ZHAN Yan-hu, LAGO E, SANTILLO C, CASTILLO A E D R C, HAO Shuai, BUONOCORE G G, CHEN Zhen-ming, XIA He-sheng, LAVORGNA M, BONACCORSO F. An anisotropic layer-by-layer carbon nanotube/boron nitride/rubber composite and its application in electromagnetic shielding [J]. Nanoscale, 2020, 12: 7782−7791. doi: 10.1039/C9NR10672C.

[25] WANASINGHE D, ASLANI F, MA Guo-wei, HABIBI D. Review of polymer composites with diverse nanofillers for electromagnetic interference shielding [J]. Nanomaterials, 2020, 10(3): 541. doi: 10.3390/nano10030541.

[26] YIN Xiao-wei, KONG Luo, ZHANG Li-tong, CHENG Lai-fei, TRAVITZKY N, GREIL P. Electromagnetic properties of Si−C−N based ceramics and composites [J]. International Materials Reviews, 2014, 59(6): 326−355. doi: 10.1179/1743280414Y.0000000037.

[27] KUMAR P, NARAYAN M U, SIKDAR A, KUMAR D T, KUMAR A, SUDARSAN V. Recent advances in polymer and polymer composites for electromagnetic interference shielding: Review and future prospects [J]. Polymer Reviews, 2019, 59(4): 687−738. doi: 10.1080/15583724.2019.1625058.

[28] GEETHA S, SATHEESH K K K, RAO C R K, VIJAYAN M, TRIVEDI D C. EMI shielding: Methods and materials—A review [J]. Journal of Applied Polymer Science, 2009, 112(4): 2073−2086. doi: 10.1002/app.29812.

[29] LIU Wen-cai, GAO Zhan-kui, PENG Xiang, WU Guo-hua, TONG Xin, XIAO Lv, WANG Xian-fei, DING Wen-jiang. Microstructural evolution and mechanical properties of as-cast and as-extruded Mg−14Li alloy with different Zn/Y and Zn/Gd addition [J]. Advanced Engineering Materials, 2020, 22(11): 2000480. doi: 10.1002/adem.202000480.

[30] ZHANG Yang, ZHANG Jie, WU Guo-hua, LIU Wen-cai, ZHANG Liang, DING Wen-jiang. Microstructure and tensile properties of as-extruded Mg−Li−Zn−Gd alloys reinforced with icosahedral quasicrystal phase [J]. Materials & Design, 2015, 66: 162−168. doi: 10.1016/j.matdes.2014.10.049.

[31] HAN G Q, SHEN J H, YE X X, CHEN B, IMAI H, KONDOH K, DU W B. The influence of CNTs on the microstructure and ductility of CNT/Mg composites [J]. Materials Letters, 2016, 181: 300−304. doi: 10.1016/j.matlet.2016.06.021.

[32] WEI Zhen, ZHENG Hai-peng, WU Rui-zhi, ZHANG Jing-huai, WU Hua-jie, JIN Si-yuan, JIAO Yun-lei, HOU Le-gan. Interface behavior and tensile properties of Mg−14Li−3Al−2Gd sheets prepared by four-layer accumulative roll bonding [J]. Journal of Manufacturing Processes, 2021, 61: 254−260. doi: 10.1016/j.jmapro.2020.11.021.

[33] LI Shu-bo, YANG Xin-yu, HOU Jiang-tao, DU Wen-bo. A review on thermal conductivity of magnesium and its alloys [J]. Journal of Magnesium and Alloys, 2020, 8(1): 78−90. doi: 10.1016/j.jma.2019.08.002.

[34] JI Qing, WANG Yang, WU Rui-zhi, WEI Zhen, MA Xiao-chun, ZHANG Jing-huai, HOU Le-gan, ZHANG Mi-lin. High specific strength Mg−Li−Zn−Er alloy processed by multi deformation processes [J]. Materials Characterization, 2020, 160: 110135. doi: 10.1016/j.matchar.2020.110135.

[35] TANG Song, XIN Tong-zheng, XU Wan-qiang, MISKOVIC D, SHA Gang, QUADIR Z, RINGER S, NOMOTO K, BIRBILIS N, FERRY M. Precipitation strengthening in an ultralight magnesium alloy [J]. Nature Communications, 2019, 10(1): 1003. doi: 10.1038/s41467-019-08954-z.

[36] GU Kan, ZENG Xiao-qin, CHEN Bin, WANG Ying-xin. Effect of double aging on mechanical properties and microstructure of EV31A alloy [J]. Transactions of Nonferrous Metals Society of China, 2021, 31(9): 2606−2614. doi: 10.1016/S1003-6326(21)65679-0.

[37] CAO Li-jie, MA Guo-rui, WANG Chun-xia, CHEN Zheng-jian, ZHANG Jia-heng. Effect of compression ratio on microstructure evolution of Mg−10%Al−1%Zn−1%Si alloy prepared by SIMA process [J]. Transactions of Nonferrous Metals Society of China, 2021, 31(9): 2597−2605. doi: 10.1016/S1003-6326(21)65678-9.

[38] LIU Chun-quan, CHEN Xian-hua, YUAN Yuan, ZHANG Wei, ZHANG Yu-sheng, PAN Fu-sheng. Altered age-hardening behavior in the ultrafine-grained surface layer of Mg−Zn−Y−Ce−Zr alloy processed by sliding friction treatment [J]. Journal of Materials Science & Technology, 2021, 78: 20−29. doi: 10.1016/j.jmst.2020.11.017.

[39] ZHAO Yang, ZHANG Ding-fei, FENG Jing-kai, CHEN Xia, DENG Tian-yu, JIANG Bin, PAN Fu-sheng. Effect of Gd addition on the age hardening response of Mg−6Zn−1Mn alloy [J]. Journal of Materials Research and Technology, 2020, 9(4): 8834−8841. doi: 10.1016/j.jmrt.2020.05.120.

[40] ZHAO Jiong, LI Zhong-quan, LIU Wen-cai, ZHANG Jie, ZHANG Liang, TIAN Ying, WU Guo-hua. Influence of heat treatment on microstructure and mechanical properties of as-cast Mg−8Li−3Al−2Zn−xY alloy with duplex structure [J]. Materials Science and Engineering A, 2016, 669: 87−94. doi: 10.1016/j.msea.2016.05.085.

[41] WANG Qing-hang, CHEN Si-yuan, JIANG Bin, JIN Zhao-yang, ZHAO Ling-yu, HE Jun-jie, ZHANG Ding-fei, HUANG Guang-sheng, PAN Fu-sheng. Grain size dependence of annealing strengthening of an extruded Mg−Gd−Zn alloy subjected to pre-compression deformation [J]. Journal of Magnesium and Alloys, 2021. doi: 10.1016/j.jma.2021.03.015.

[42] NIE K B, WANG X J, DENG K. K, HU X. S, WU K. Magnesium matrix composite reinforced by nanoparticles—A review [J]. Journal of Magnesium and Alloys, 2021, 9(1): 57−77. doi: 10.1016/j.jma.2020.08.018.

[43] WANG Jing-feng, GAO Shan, ZHAO Liang, LIANG Hao, HU Yan-bo, PAN Fu-sheng. Effects of Y on mechanical properties and damping capacity of ZK60 magnesium alloys [J]. Transactions of Nonferrous Metals Society of China, 2010, 20: s366−s370. doi: 10.1016/S1003-6326(10) 60499-2.

[44] CHE Chao-jie, CHENG Li-ren, TONG Li-bo, CAI Zhong-yi, ZHANG Hong-jie. The effect of Gd and Zn additions on microstructures and mechanical properties of Mg−4Sm−3Nd−Zr alloy [J]. Journal of Alloys and Compounds, 2017, 706: 526−537. doi: 10.1016/j.jallcom.2017.02.269.

[45] JIANG Yan, CHEN Yu-an, GAO Jun-jie. Comparative study regarding the effect of Al, Zn, and Gd on the microstructure and mechanical properties of Mg alloy Mg−Sn−Li [J]. Materials & Design, 2016, 105: 34−40. doi: 10.1016/j.matdes.2016.05.061.

[46] RUDAJEVOVÁ A, KÚDELA S, STANĚK M, LUKÁČ P. Thermal properties of Mg−Li and Mg−Li−Al alloys [J]. Materials Science and Technology, 2013, 19(8): 1097−1100, doi: 10.1179/026708303225004648.

[47] ZHANG Ding-fei, SHI Guo-liang, ZHAO Xia-bing, QI Fu-gang. Microstructure evolution and mechanical properties of Mg−*x*%Zn−1%Mn (*x*=4, 5, 6, 7, 8, 9) wrought magnesium alloys [J]. Transactions of Nonferrous Metals Society of China, 2011, 21: 15−25. doi: 10.1016/S1003-6326(11)60672-9.

[48] SONG K, PAN F S, CHEN X H, TANG A, PAN H, LUO S. Effect of Zn content on electromagnetic interference shielding effectiveness of Mg−Zn alloys [J]. Materials Research Innovations, 2014, 18(S4): 193−197. doi: 10.1179/1432891714Z.000000000676.

[49] LUO Zhu, CHEN Xian-hua, SONG Kai, LIU Chun-quan, DAI Yan, ZHAO Di, PAN Fu-sheng. Effect of alloying element on electromagnetic interference shielding effectiveness of binary magnesium alloys [J]. Acta Metallurgica Sinica (English Letters), 2019, 32(7): 817−824. doi: 10.1007/s40195-019-00887-2.

[50] CHEN Xian-hua, GENG Yu-xiao, PAN Fu-sheng. Microstructure, mechanical properties and electromagnetic shielding effectiveness of Mg−Y−Zr−Nd alloy [J]. Rare Metal Materials and Engineering, 2016, 45(1): 13−17. doi: 10.1016/S1875-5372(16)30037-6.

[51] Yang Chu-bin, PAN Fu-sheng, CHEN Xian-hua, LUO Ning. Effects of Sm addition on electromagnetic interference shielding property of Mg−Zn−Zr alloys [J]. Applied Physics A, 2017, 123(6): 400. doi: 10.1007/s00339-017-1011-5.

[52] LIU Li-zi, CHEN Xian-hua, WANG Jing-feng, QIAO Li-ying, GAO Shang-yu, SONG Kai, ZHAO Chao-yue, LIU Xiao-fang, ZHAO Di, PAN Fu-sheng. Effects of Y and Zn additions on electrical conductivity and electromagnetic shielding effectiveness of Mg−Y−Zn alloys [J]. Journal of Materials Science & Technology, 2019, 35(6): 1074−1080. doi: 10.1016/j.jmst.2018.12.010.

[53] XU C, NAKATA T, QIAO X G, ZHENG M Y, WU K, KAMADO S. Ageing behavior of extruded Mg−8.2Gd−3.8Y−1.0Zn−0.4Zr (wt.%) alloy containing LPSO phase and gamma' precipitates [J]. Scientific Reports, 2017, 7: 43391, doi: 10.1038/srep43391.

[54] MAURYA R, MITTAL D, BALANI K. Effect of heat-treatment on microstructure, mechanical and tribological properties of Mg−Li−Al based alloy [J]. Journal of Materials Research and Technology, 2020, 9(3): 4749−4762. doi: 10.1016/j.jmrt.2020.02.101.

[55] PENG Q Z, ZHOU H T, ZHONG F H, DING H B, ZHOU X, LIU R R, XIE T, PENG Y. Effects of homogenization treatment on the microstructure and mechanical properties of Mg−8Li−3Al−Y alloy [J]. Materials & Design, 2015, 66: 566−574. doi: 10.1016/j.matdes.2014.03.046.

[56] WU Hua-jie, WANG Tian-zi, WU Rui-zhi, HOU Le-gan, ZHANG Jing-huai, LI Xin-lin, ZHANG Mi-lin. Effects of annealing process on the interface of alternate α/β Mg−Li composite sheets prepared by accumulative roll bonding [J]. Journal of Materials Processing Technology, 2018, 254: 265−276. doi: 10.1016/j.jmatprotec.2017.11.033.

[57] CHEN Xian-hua, LIU Juan, ZHANG Zhi-hua, PAN Fu-sheng. Effect of heat treatment on electromagnetic shielding effectiveness of ZK60 magnesium alloy [J]. Materials & Design, 2012, 42: 327−333. doi: 10.1016/j.matdes.2012.05.061.

[58] CHEN Xian-hua, LIU Juan, PAN Fu-sheng. Enhanced electromagnetic interference shielding in ZK60 magnesium alloy by aging precipitation [J]. Journal of Physics and Chemistry of Solids, 2013, 74(6): 872−878. doi: 10.1016/j.jpcs.2013.02.003.

[59] CHEN X H, LIU L Z, PAN F S, QIAO L. Mechanical properties and electromagnetic shielding effectiveness of ZK60 magnesium alloy subjected to cold rolling and aging [J]. Materials Research Innovations, 2014, 18(S4): 187−192. doi: 10.1179/1432891714Z. 000000000672.

[60] WANG Jia-hao, JIN Si-yuan, WU Rui-zhi, XU Lin, ZHANG Jing-huai, FENG, Jing, HOU Le-gan, JIAO Yun-lei. Improvement of electromagnetic shielding properties for Mg−8Li−6Y−2Zn alloy by heat treatment and hot rolling [J]. Journal of Materials Science: Materials in Electronics, 2020, 31: 17249−17257. doi: 10.1007/s10854-020-04279-6.

[61] GAO Shang-yu, CHEN Xian-hua, PAN Fu-sheng, SONG Kai, ZHAO Chao-yuee, LIU Li-zi, LIU Xiao-fang, ZHAO Di. Effect of secondary phase on the electromagnetic shielding effectiveness of magnesium alloy [J]. Scientific Reports, 2018, 8(1): 1625. doi: 10.1038/s41598-018-19933-7.

[62] LIU Wei, ZENG Zhuoran, HOU Hua, ZHANG Jin-shan, ZHU Yu-man. Dynamic precipitation behavior and mechanical properties of hot-extruded Mg89Y4Zn2Li5 alloys with different extrusion ratio and speed [J]. Materials Science and Engineering A, 2020, 798: 140121, doi: 10.1016/j.msea.2020.140121.

[63] JIANG Han-si, QIAO Xiao-guang, XU Chao, KAMADO S, WU Kun, ZHENG Ming-yi. Influence of size and distribution of W phase on strength and ductility of high strength Mg−5.1Zn−3.2Y−0.4Zr−0.4Ca alloy processed by indirect extrusion [J]. Journal of Materials Science & Technology, 2018, 34(2): 277−283, doi: 10.1016/j.jmst.2017.11.022.

[64] CHEN Chao, CHEN Ji-hua, YAN Hong-ge, SU Bin, SONG Min, ZHU Su-qin. Dynamic precipitation, microstructure and mechanical properties of Mg−5Zn−1Mn alloy sheets prepared by high strain-rate rolling [J]. Materials & Design, 2016, 100: 58−66. doi: 10.1016/j.matdes.2016.03.129.

[65] WANG Bao-jie, XU Kai, XU Dao-kui, CAI Xiang, QIAO Yan-xin, SHENG Li-yuan. Anisotropic corrosion behavior of hot-rolled Mg−8wt.%Li alloy [J]. Journal of Materials Science & Technology, 2020, 53: 102−111. doi: 10.1016/j.jmst.2020.04.029.

[66] KOCICH R, MACHÁČKOVÁ A, FOJTÍK F. Comparison of strain and stress conditions in conventional and ARB rolling processes [J]. International Journal of Mechanical Sciences, 2012, 64(1): 54−61. doi: 10.1016/j.ijmecsci.2012.08.003.

[67] LIU T, WANG Y D, WU S D, LIN P R, HUANG C X, JIANG C B, LI S X. Textures and mechanical behavior of Mg−3.3%Li alloy after ECAP [J]. Scripta Materialia, 2004, 51(11): 1057−1061. doi: 10.1016/j.scriptamat.2004.08.007.

[68] SONG K, PAN F S, CHEN X H, ZHANG Z H, TANG A T, SHE J, YU Z W, PAN H C, XU X Y. Effect of texture on the electromagnetic shielding property of magnesium alloy [J]. Materials Letters, 2015, 157: 73−76. doi: 10.1016/j.matlet.2015.05.017.

[69] WU Zhao-xuan, AHMAD R, YIN Bing-lun, SANDLÖBES S, CURTIN W A. Mechanistic origin and prediction of enhanced ductility in magnesium alloys [J]. Science, 2018, 359: 447−451. doi: 10.1126/science.aap8716.

[70] WANG Dan, LIU Shu-juan, WU Rui-zhi, ZHANG Shun, WANG Yang, WU Hua-jie, ZHANG Jing-huai, HOU Le-gan. Synergistically improved damping, elastic modulus and mechanical properties of rolled Mg−8Li−4Y−2Er−2Zn−0.6Zr alloy with twins and long-period stacking ordered phase [J]. Journal of Alloys and Compounds, 2021, 881: 160663. doi: 10.1016/j.jallcom.2021.160663.

[71] WANG Jia-hao, WU Rui-zhi, FENG Jing, ZHANG Jing-huai, HOU Le-gan, ZHANG Mi-lin. Influence of rolling strain on electromagnetic shielding property and mechanical properties of dual-phase Mg−9Li alloy [J]. Materials Characterization 2019, 157: 109924. doi: 10.1016/j.matchar.2019.109924.

[72] XIAO X F, ZHANG X, LI B C, ZHANG Z M, GUO R L. Effects of extrusion deformation on electromagnetic shielding properties of Mg−Gd−Y−Zn−Zr rare earth magnesium alloy [J]. Ordnance Material Science and Engineering, 2017, 40(2): 69−72. doi: 10.14024/j.cnki.1004-244x.20170303.027.

[73] CHEN Xian-hua, LIU Li-zi, PAN Fu-sheng, MAO Jian-jun, XU Xiao-yang, YAN Tao. Microstructure, electromagnetic shielding effectiveness and mechanical properties of Mg−Zn−Cu−Zr alloys [J]. Materials Science and Engineering B, 2015, 197: 67−74. doi: 10.1016/j.mseb.2015.03.012.

[74] ZHAN Mei-yan, ZHANG Wei-wen, ZHANG Da-tong, Production of Mg−Al−Zn magnesium alloy sheets with ultrafine-grain microstructure by accumulative roll-bonding [J]. Transactions of Nonferrous Metals Society of China, 2011, 21: 991−997. doi: 10.1016/S1003-6326(11) 60811-X.

[75] ETEMAD A, DINI G, SCHWARZ S. Accumulative roll bonding (ARB)-processed high-manganese twinning induced plasticity (TWIP) steel with extraordinary strength and reasonable ductility [J]. Materials Science and Engineering A, 2019, 742: 27−32. doi: 10.1016/j.msea.2018.10.119.

[76] EBRAHIMI S H S, DEHGHANI K, AGHAZADEH J, GHASEMIAN M B, ZANGENEH S. Investigation on microstructure and mechanical properties of Al/Al−Zn−Mg−Cu laminated composite fabricated by accumulative roll bonding (ARB) process [J]. Materials Science and Engineering A, 2018, 718: 311−320. doi: 10.1016/j.msea.2018.01.130.

[77] MANSOURI H, EGHBALI B, AFRAND M. Producing multi-layer composite of stainless steel/aluminum/copper by accumulative roll bonding (ARB) process [J]. Journal of Manufacturing Processes, 2019, 46: 298−303. doi: 10.1016/j.jmapro.2019.08.025.

[78] LEU B, SAVAGE D J, WANG J, ALAM M E, MARA N A, KUMAR M A, CARPENTER J S, VOGEL S C, KNEZEVIC M, DECKER R, BEYERLEIN I J. Processing of dilute Mg−Zn−Mn−Ca alloy/Nb multilayers by accumulative roll bonding [J]. Advanced Engineering Materials, 2019, 22(1): 1900673. doi: 10.1002/adem. 201900673.

[79] WANG Jia-hao, XU Lin, WU Rui-zhi, FENG Jing, ZHANG Jing-huai HOU Le-gan, ZHANG Mi-lin. Enhanced electromagnetic interference shielding in a duplex-phase Mg−9Li−3Al−1Zn alloy processed by accumulative roll bonding [J]. Acta Metallurgica Sinica (English Letters), 2020, 33(4): 490−499. doi: 10.1007/s40195-020-01017-z.

[80] WANG X J, HU X S, WANG Y Q, NIE K B, WU K, ZHENG M Y. Microstructure evolutions of SiC_p/AZ91 Mg matrix composites during hot compression [J]. Materials Science and Engineering A, 2013, 559: 139−146. doi: 10.1016/j.msea.2012.08.054.

[81] XU Tian-cai, YANG Yan, PENG Xiao-dong, SONG Jiang-feng, PAN Fu-sheng. Overview of advancement and development trend on magnesium alloy [J]. Journal of Magnesium and Alloys, 2019, 7(3): 536−544. doi: 10.1016/j.jma.2019.08.001.

[82] GUPTA M, WONG W L E. Magnesium-based nanocomposites: Lightweight materials of the future [J]. Materials Characterization, 2015, 105: 30−46. doi: 10.1016/j.matchar.2015.04.015.

[83] HU Xiao-shi, SUN Zhen-ming, ZHANG Chun-lei, WANG Xiao-jun, WU Kun. Microstructure and mechanical properties of bio-inspired Cf/Ti/Mg laminated composites [J]. Journal of Magnesium and Alloys, 2018, 6(2): 164−170. doi: 10.1016/j.jma.2018.04.005.

[84] HOU Jiang-tao, DU Wen-bo, WANG Zhao-hui, LI Shu-bo, LIU Ke, DU Xian. Combination of enhanced thermal conductivity and strength of MWCNTs reinforced Mg−6Zn matrix composite [J]. Journal of Alloys and Compounds, 2020, 838: 155573. doi: 10.1016/j.jallcom.2020.155573.

[85] WANG Yang, LIAO Yang, WU Rui-zhi, TURAKHODJAEV N, CHEN Hong-tao, ZHANG Jing-huai, ZHANG Mi-lin, MARDONAKULOV S. Microstructure and mechanical properties of ultra-lightweight Mg−Li−Al/Al−Li composite produced by accumulative roll bonding at ambient temperature [J]. Materials Science and Engineering A, 2020, 787: 139494. doi: 10.1016/j.msea.2020.139494.

[86] RAHMATABADI D, PAHLAVANI M, GHOLAMI M D, MARZBANRAD J, HASHEMI R. Production of Al/Mg−Li composite by the accumulative roll bonding process [J]. Journal of Materials Research and Technology, 2020, 9(4): 7880−7886. doi: 10.1016/j.jmrt.2020.05.084.

[87] LI G H, ZHOU L, ZHANG H F, GUO G Z, LUO S F, GUO

N. Evolution of grain structure, texture and mechanical properties of a Mg−Zn−Zr alloy in bobbin friction stir welding [J]. Materials Science and Engineering A, 2021, 799: 140267. doi: 10.1016/j.msea.2020.140267.

[88] LU N N, WANG X J, MENG L L, DING C, LIU W Q, SHI H L, HU X S, WU K. Electromagnetic interference shielding effectiveness of magnesium alloy−fly ash composites [J]. Journal of Alloys and Compounds, 2015, 650: 871−877. doi: 10.1016/j.jallcom.2015.08.019.

[89] PANDEY R, TEKUMALLA S, GUPTA M. Magnesium-iron micro-composite for enhanced shielding of electromagnetic pollution [J]. Composites Part B: Engineering, 2019, 163: 150−157. doi: 10.1016/j.compositesb.2018.11.038.

[90] PANDEY R, TEKUMALLA S, GUPTA M. Enhanced (X-band) microwave shielding properties of pure magnesium by addition of diamagnetic titanium micro-particulates [J]. Journal of Alloys and Compounds, 2019, 770: 473−482. doi: 10.1016/j.jallcom.2018.08.147.

[91] WANG Jia-hao, LI Yang WU Rui-zhi, XU Lin, ZHANG Zhen, FENG Jing, ZHANG Jing-huai, HOU Le-gan, JIAO Yun-lei. X-band shielding properties of Mg−9Li matrix composite containing $Ni_{0.4}Zn_{0.4}Co_{0.2}Fe_2O_4$ fabricated by multi-layer composite rolling [J]. Journal of Alloys and Compounds, 2020, 843: 156053. doi: 10.1016/j.jallcom.2020.156053.

[92] WANG Jia-hao, XU Lin, WU Rui-zhi, AN Di, WEI Zhen, WANG Jia-xiu, FENG Jing, ZHANG Jing-huai, HOU Le-gan, LIU Mei-duo. Simultaneous achievement of high electromagnetic shielding effectiveness (X-band) and strength in Mg−Li−Zn−Gd/MWCNTs composite [J]. Journal of Alloys and Compounds, 2021, 882: 160524. doi: 10.1016/j.jallcom.2021.160524.

电磁屏蔽 Mg 基材料及其加工工艺的研究进展

王佳豪[1]，巫瑞智[1,2]，冯 静[1]，张景怀[1]，侯乐干[1]，刘美多[3]

1. 哈尔滨工程大学 超轻材料与表面技术教育部重点实验室，哈尔滨 150001；
2. 黑河学院 理学院，黑河 164300；
3. 黑龙江工业学院 环境工程部，鸡西 158100

摘 要：在轻质电磁干扰(EMI)屏蔽结构材料方面，Mg 基材料已被证明是一种很好的备选材料，因为其具有优异的特性(例如：低密度、高比强度、良好的导电性和优异的 EMI 屏蔽性能)以及在电子、汽车和航空航天等工业轻量化领域的广泛应用。通过合金化、热处理、塑性变形和复合加工等工艺，可以获得具有可定制特性的 Mg 基材料，这在设计用于 EMI 屏蔽的材料中起到关键作用。本文综述了近几十年来 Mg 基材料 EMI 屏蔽性能的研究及其 EMI 屏蔽机制，重点介绍了合金化、热处理、塑性变形和复合加工工艺对 Mg 基材料 EMI 屏蔽性能的影响。最后，提供了结论和未来展望。

关键词：Mg；电磁干扰屏蔽；合金化；热处理；塑性变形；复合加工

(Edited by Bing YANG)